Mostafa Esmaeili Shayan, Gholamhassan Najafi, Barat Ghobadian, Shiva Gorjian, Rizalman Mamat, and Mohd Fairusham Ghazali, "Multi-Microgrid Optimization and Energy Management under Boost Voltage Converter with Markov Prediction Chain and Dynamic Decision Algorithm." Renewable Energy, 201, 2022, 179–89.

The publisher's version is available at:

https://doi.org/10.1016/j.renene.2022.11.006

Multi-Microgrid Optimal Hybrid Energy Management Under Boost voltage DC-DC with Predictive Analytics and Dynamic Decision Algorithm

Mostafa Esmaeili Shayan[1], Gholamhassan Najafi[*2],Barat Ghobadian[3], Shiva Gorjian[4], Rizalman Mamat[5], Mohd Fairusham Ghazali[6]

[1] Department of Biosystem Engineering, Tarbiat Modares University, Tehran, Iran, E.mostafa@modares.ac.ir

[2] Department of Biosystem Engineering, Tarbiat Modares University, Tehran, Iran, g.najafi@modares.ac.ir

[3] Department of Biosystem Engineering, Tarbiat Modares University, Tehran, Iran, ghobadian@modares.ac.ir

[4] Department of Biosystem Engineering, Tarbiat Modares University, Tehran, Iran, gorjian@modares.ac.ir

[5] Center for Research in Advanced Fluid and Process, University Malaysia Pahang, Lebuhraya Tun Razak, Gambang, Kuantan 26300, Pahang, Malaysiaxz, rizalman@ump.edu.my

[6] Center for Research in Advanced Fluid and Process, University Malaysia Pahang, Lebuhraya Tun Razak, Gambang, Kuantan 26300, Pahang, Malaysiaxz, fairusham@ump.edu.my

**Corresponding Author: g.najafi@modares.ac.ir*

Abstract

Covering operational energy consumption and embodied energy, replacing embodied greenhouse gas (GHG) emissions in building materials, and knowing national energy resources are required. In this study, the importance of investigating the stochastic nature of weather-dependent renewable energies is well documented. The management of the hybrid renewable energy system (HRES) was built and assessed, utilizing a decision-making algorithm and 13 case studies. When the proportion of renewable energy is at 24% and the average daily fossil fuel usage is 1.11 liters per year, the HRES generates 1697 kWh per year with a net present value (NPV) of 553,68 USD, with a rate of return (IRR) of 21.4%, and a payback period (PP) of 15.7 years. With a renewable energy share of 54%, fossil fuel consumption dropped to 0.69 liters per year, while yearly energy output was comparable to 1,652 kWh per year, with an IRR of 19.5% and a PP of 17.6 years. To achieve zero greenhouse gas emissions, HRES Management employs 100% renewable energy sources to generate 1933 kWh per year at a net present value of -372.09 US dollars. This scenario is economically possible if the renewable energy feed-in tariff exceeds 0.06 USD.

Keywords: Renewable Energies; Greenhouse Gas (GHG); Hybrid Renewable Energy System (HRES); Decision-Making Algorithm; Fossil Fuel.

Nomenclature

Symbols

P	Power
D	Demand
I	Electric Current, Solar Irradiance
Q	Irradiance
T	Temperature
V	Voltage
W,S	Wind Speed

Subscript

min	Minimum
ci	Cut-In
co	Cut-Out
dy	Dynamic
max	Maximum
s	Level
yr	Yearly

Greek Symbols

η	Efficiency
Δt	Sampling Time Interval
β	Slope Angle
γ	Azimuth Angle
α	Power Temperature Coefficient
δ	Coefficients of the Autoregressive Model
ε	Forecast Errors
μ	Coefficients of The Moving Averages

Acronyms

AC	Alternating Current
ARMA	Autoregressive Moving Average
BESS	Battery Energy Storage Systems
COE	Cost of Electricity
DC	Direct Current
DE	Diesel Generator
DER	Distributed Energy Resources
ED	Economic Dispatch
HERS	Hybrid Renewable Energy System
IRR	Internal Rate of Return
LCOE	Levelized Cost of Energy
MG	Microgrid
NCF	Net Cash Flow
NPV	Net Present Value
PID	Proportional Integral Derivative
PV	Photovoltaic
RES	Renewable Energy Systems
ROI	Return on Investment
SOC	State of charge
STC	Standard Test Conditions
SUC	Stochastic Unit Commitment
UC	Unit Commitment
WT	Wind Turbine
ZEB	Zero-Energy Building

1. Introduction

Due to limited resources, traditional energy systems can't keep up with population expansion and industrialisation. According to the world energy organization, fossil fuel reserves, which provide 79% of the world's basic energy, are swiftly diminishing, with 57% of them used in transportation. As energy demand grows and supply falls due to environmental concerns, countries' economies will become unstable. Local and sustainable energy sources are crucial.

Renewable energy fluctuates geographically. Photovoltaic and wind energy systems don't work at night. Design and integration of photovoltaic-wind hybrid systems, as well as efficient storage and backup systems, can boost the willingness to employ renewable systems and control the energy cycle. This technique supports local or household renewable energy consumption while building the basis for large-scale power generation [1]. Investing in solar and wind systems is expensive compared to fossil fuels [2]. Combining conventional and renewable energy sources improves cost-effectiveness and reliability [3]. A small-grid renewable energy management solution incorporates multiple yet complimentary methods [4]. With the rising usage of hybrid renewable energy systems, especially in distant power supplies, cost-and reliability-optimal design is crucial. Energy researchers have spent decades trying to control renewable systems [5]. Compared to standalone systems, integrated renewable energy systems are powerful. Hourly electricity demand from 2,000 Swedish houses [6]. P-GA-PSO method was used in a research for energy management and efficiency. The result was the use of an innovative method in energy price estimation [7]. Positive feedback between central power generation and house investments in a hybrid solar system and batteries has changed the market to single-family dwellings [8]. A 2018 research advocated the intelligent control of a solar system utilizing fuzzy logic [9]. In 2021, another research suggests an intelligent control approach for a direct-connected, tracking photovoltaic solar power plant [10]. Recent research focuses on hybrid networks and real-time algorithms [11]. Lee et al. (2018) explored a grid-connected system for regulating consumption and peak correction in Japanese homes [12]. In another research, real-time optimization was done based on dynamic programming and two-dimensional algorithm. A technique for optimizing energy management combining real-time and anticipated data has produced the desired outcome [13]. Coordination of solar array, battery storage, and capacitor network integration was also studied. Invention clustering and solar battery development are also studied [14]. Elsheikh et al. developed a hybrid energy control system in 2019. This system controls electricity generation to maximize profits and minimize operational expenses. Environment determined the control situation. The power generation system predicted load distribution and profit-maximizing environmental circumstances. Operating profit, imbalance factor, effective operation forecasts, and time delay were used to assess the suggested system [15].

Yang et al. developed a hybrid renewable energy forecasting system in 2020. This system managed alternating and random renewable energy flow to increase load dependability. Only the axial part of the flow needs to be controlled and the disturbance control is simple [16]. YiHe et al. implemented battery for multi-objective algorithms for the storage and management of electric energy. The results shown that energy estimation can be performed with high precision using meteorological and anticipated data, and the field evaluation of the decision-making method based on voltage control and Non-dominated Sorting Genetic Algorithm-II was effective[17]. A typical control includes integral-derivative PID control, passivity-based control connection, sliding state control, and regular sliding state fraction control. They showed that PID's active power error is small. This study tested dSpace-based hardware under different situations [18]. In a recent study, a control system with a Peak shaving technique was implemented employing HRES and BESS. The technological gap was narrowed by conducting detailed benefit evaluations based on the equivalent coefficient and by including a storage mechanism to accommodate fluctuating solar radiation and ambient temperature [19]. Pravin et al. created a framework for combining renewable energy sources with a fuel cell system in 2020. This study relied on a storage technology to deal for solar and wind's alternating nature. Over a week, a scheduling layer that gives a precise plan of the ideal proportion of available electricity sources was explored [20]. The correct operation of the power generation system was recorded by the installed modifier's production decision-making. The results showed that the envisaged control system could generate a renewable energy-balanced load. Without a hardware model, validation is impossible [21]. Dong et al. implemented the forecast control model's maximum renewable energy cooling, heating, and combined power system performance in 2020. Users can use the system's produced load for heating or cooling. Based on the energy storage unit's dynamic features, a prediction-error energy optimization model is proposed. Target performance is an approach to optimize system running expenses. Optimizing each device's output minimizes operational costs under maximum forecast error [22]. Nogharian and Kofiger designed hybrid wind, solar, and battery renewable energy systems in 2020 using switch mechanisms. This system uses adaptive control to fulfill total electricity demand under automated switching. The suggested control law only considered velocity and angular flow, not wind energy. The simulation results demonstrated the suggested method's performance in a typical hybrid energy system [23]. In a series of studies, a novel optimization strategy for hybrid renewable systems was employed. The results shown that the simulated annealing process can achieve self-consumption average values of 0.93 and that the proposal might reduce CO_2 emissions by 2,838 tons. Additionally, Green energy systems will minimize annual nonrenewable energy use by 553 MWh[24].

According to a research review, governments throughout the world are trying to solve the problem of sustainable energy supply by passing environmental laws and regulations and different incentives based on technological, economic, and environmental criteria [25]. In different climatic conditions, research was undertaken with the goal of reducing power costs and meeting all energy demands with renewable sources. The results indicated that the system's overall exergy efficiency ranges from 13 to 16 percent. In the European region, the specific expenses vary considerably by month and place. The southernmost site has the LCOE at 0.289 €/kWh and heat products at 0.320 €/kWh_{ex}. The comparison results demonstrate that the HRES is cost-effective [26]. In a comparative research, Shabestari et al. conducted a technical and economic evaluation using nine linear regression machine learning approaches. Using renewable energy as a source, CO_2 emissions are reduced by an average of 16-28% compared to the pure grid. The results showed that the summer outages in Iran by 2040 are estimated to exceed 90 hours per year, and the optimized system has an energy cost of $0.06/kWh and a renewable fraction of more than 15% [27]. Existing studies can't identify the economic magnitude of integrated renewable energy systems focusing on the energy controller. This study uses vertical wind turbines, solar systems, and a diesel generator (DE) as backup energy sources. A battery bank also stores energy. Batteries store extra renewable energy. When renewable energy can't fulfill demand, a backup battery is employed. The generator ensures electricity grid quality when other units' production is low or demand is high.

In this study, the importance of investigating the stochastic nature of weather-dependent renewable energies is well documented. Combining the use of dynamic decision algorithm in Markov processes to represent the uncertainty of wind power and photovoltaic unit in a Stochastic Unit Commitment (SUC) and Economic Dispatch (ED) situation and applying the Autoregressive Moving Average (ARMA) method to forecast the demand for green cottages Microgrid (MG) is the primary innovation of this study. We introduce uncertainty and stochasticity to the management of the MG scheduling issue by using these stochastic models. The viability of this method is supported by empirical evidence.

2. Materials and Methods

The increase in penetration of renewable energy sources based on weather and stochastic has definitely increased the uncertainties in energy in the hybrid system and there is a need to design a prior demand algorithm, manage and control available energy resources, model RESs and optimize resources on cheap demand response. Renewable energy sources in the world are very vast. In the meantime, Iran has available and diverse sources of energy. The test site for the systems is located in Tehran at 35° 42' 55.0728" North and 51° 24' 15.6328" East. The height of the green home is 1352 meters above sea level. The temperature varies from -1.1 degrees Celsius to +42.7 degrees Celsius. In the regions of Iran's central belt, solar radiation is favorable and in the range of 4.99 kWh/m^2. The average annual ambient temperature, according to meteorological data, is 21.2 degrees Celsius. In this research, the power supply of a green cottage with renewable energy sources was designed using linear program control system and smart grid. The solar-wind hybrid renewable energy conversion system was designed, fabricated and evaluated with the support of DE.

The Real-time HRES system performs the task of receiving data to managing and optimizing the demand of the green cottage in three stages. The first stage includes modeling the MATLAB Simulink package. The obtained results are essential for fabrication HRES. The second stage used Proteus Design Suite to design and develop the system's electronic circuits. Real-time simulations of electronic circuits are used to study and analyze their behavior. During this stage, the microcontroller is programmed with a dynamic decision-making algorithm. Finally, a green cottage uses electronic circuits and dynamic decision algorithm. Any difference between the first and second stage results has been evaluated and solved. The third stage builds the control system for the green cottage's electricity. With real environment data for a year, the system with DE support achieves the desired critical conditions and successfully manages energy, optimizing available energy resources. Figure 1 shows the outside of the prototype system subsystems that are connected to each other.

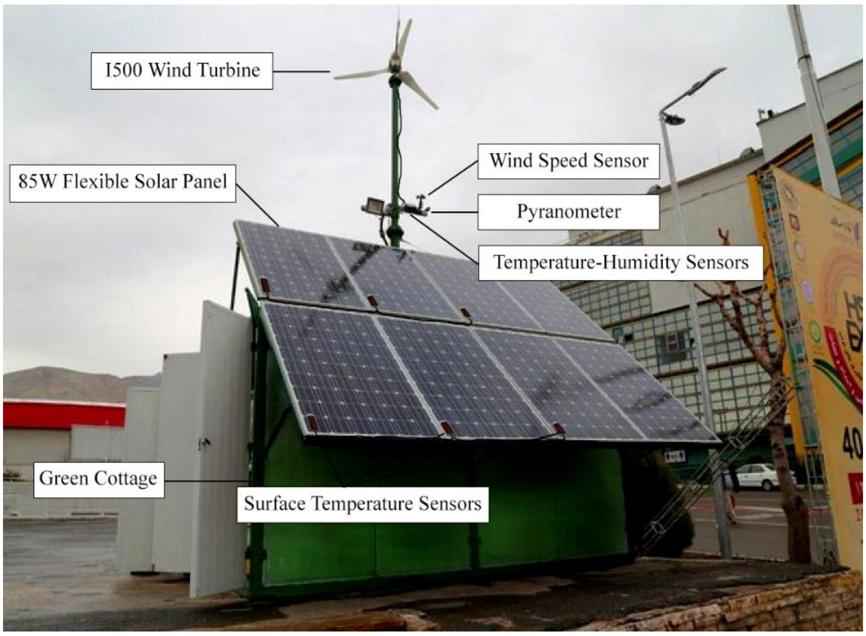

Figure 1. the RES and control equipment's for a green cottage MG.

The HRES components include electronic circuits, solar and wind subsystems, charge controller, battery bank, sensors, preparation circuits, safety circuits, converters, voltage intervention circuits, relay switching circuits, inverter and computer. Integration and fabrication of system real-time environmental testing are being conducted. Meteorological data is anticipated by the measuring instrument and each subsystem's capacity to generate electricity. Continuously managing the process of charging or discharging the battery source, the real-time management system offers 7 to 12 volts and 12 to 15 volts output voltages from renewable sources up to 230 volts. The control system gathered environmental data every hour for a whole year (8760 hours) and recorded it in LabVIEW using a USB4711 converter. A smart controller handles both energy and hybridization. Figure 2 shows the intervention model, which is based on voltage and the hardware of the control system. The MG comprised of a collection of linked loads and distributed energy resources (DERs), Like dispatchable elements such as DE, and some WT and/or PV as weather-dependent RESs. Consideration is given to battery energy storage systems (BESS) functioning as some controllable and independent units. MG can meet the load demand of green cottage off-grid or stand-alone.

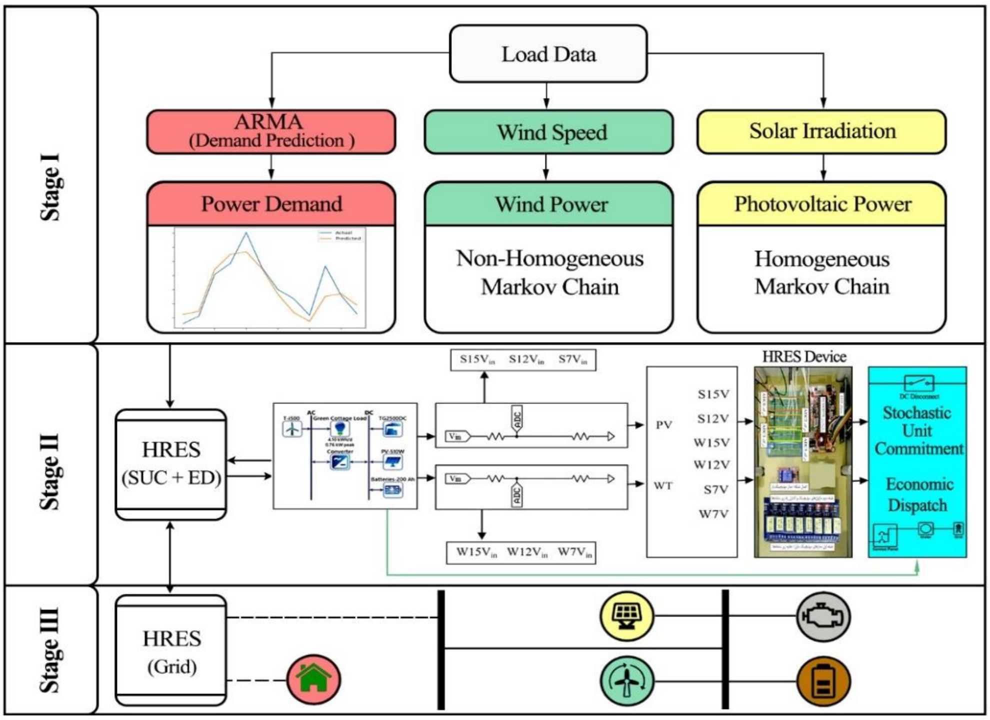

Figure 2. The predictive analytics and dynamic decision algorithm of HRES voltage control.

In the first stage, meteorological data is received through environmental sensors and access to historical data is provided. At the same time, the green cottage demand curve is predicted and modeled through ARMA. Since RESs are based on stochastic nature, the Marko process is solved as a multi-dimensional dependence for the uncertainty of renewable sources of solar energy (homogeneous) and wind energy (non-homogeneous). In the second stage, by solving the models and accessing the voltage controller in the smart HRES, the SUC and ED models are solved to cover the low-cost response to the electricity demand of the green cottage. It is believed that the conventional generating units (DE) and the BESS can compensate for demand forecast errors. The aforementioned criteria ensure that the green cottage MG can operate reliably on the island. In order to assure that this is the case, dependability requirements are added into the optimization problem. The voltage switch interfaces with the circuit breaker and power source controller to activate. Each renewable energy source's output is optimized based on controller calculations. The hybrid paradigm uses distribution control to manage subsystems in real time. In the third stage, the intelligent HRES system, using SUC and ED models in real-time with uncertainty in supply and while providing warnings for the presence of DE and BESS charging, supplies the electricity demand of green cottage MG in the form of demand side management. Then, the operating costs are reduced by optimization issues involving the determination of DE start-up time should be minimal. Real-time system control might be centralized, distributed, or hybrid. The HRES determines optimal energy performance in all three control paradigms. The centralization paradigm monitors all regulated output voltages and signals on the PIC16F18877. The signals are chosen after the renewable electricity is ready. Fig. 3 shows the system's dynamic decision algorithm. The algorithm looks at situations that allow solar and wind to charge the green cottage's MG or the BESS.

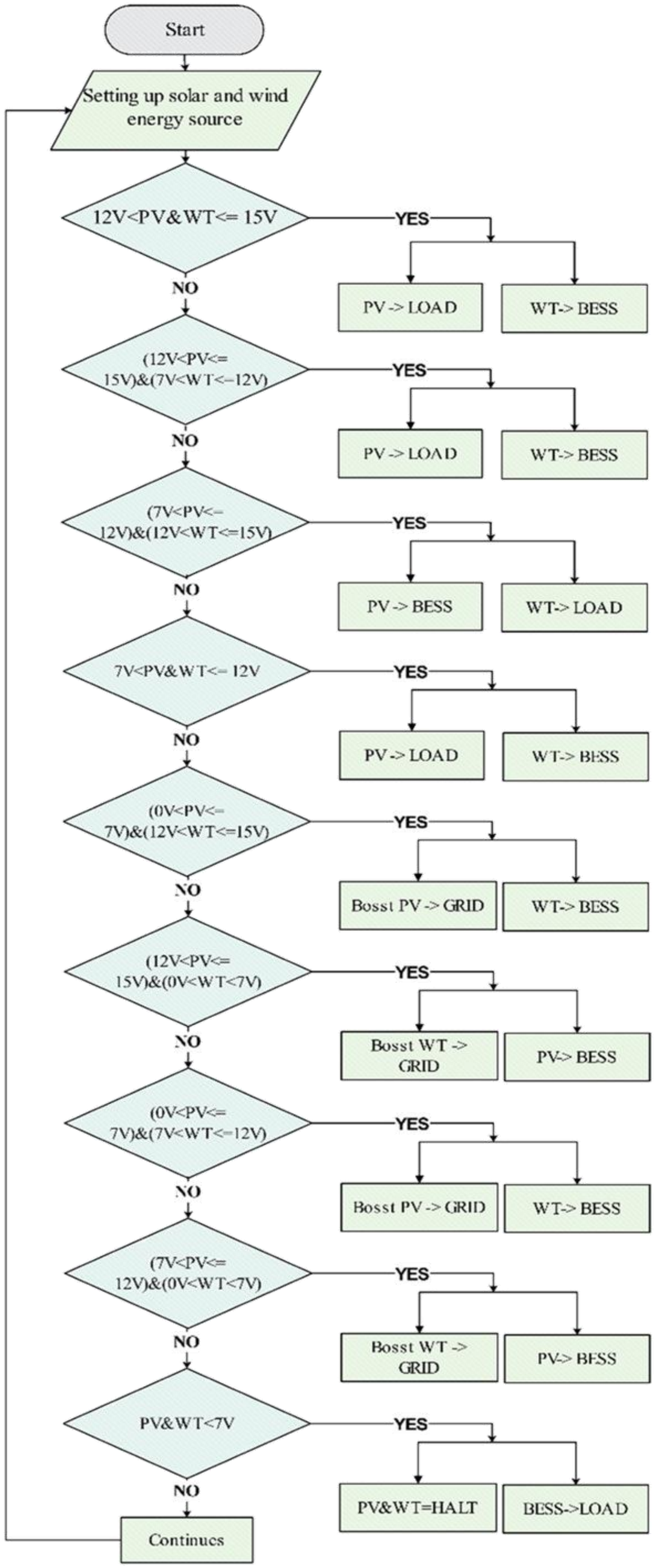

Figure 3. Algorithm for green cottage MG management and optimization.

The PIC16F18877 is coupled to 17 relays that control energy through 8 battery decision relays, 8 voltage switching relays, and 1 relay connected to the diesel generator's on/off starter. The microprocessor sends 5 volts to the relays and operates energy optimization and hybridization. In the absence of renewable energy sources, batteries B and A drain intermittently by 40% of SOC. If the battery bank goes below 40% and there is no renewable power source, the DE control system charges the batteries. After charging the battery bank or using renewable energy, the DE is shut off. To calculate the ampere-hour of a 12-volt battery, use two 100-watt bulbs with a total consumption of 10 watts and a 175-watt bulb with a total consumption of 7.5 watts. This may be used with LED daytime running lights ranging from 5 to 10 watts. The lighting portion consumes 2.29 ampere-hours each day before the inverter and 11.45 ampere-hours if all three lamps are active for 5 hours. Therefore, by summing up the load consumers, the total power required for the green cottage was estimated to be 1.06 kW to 2.5 kW. Table 1 shows the cottage's electric customers.

Table 1. Electricity consumers in green cottage [28].

Section	Wattage (W)	Time (Hours)	Ampere Hourly (Ah)
Illumination and Light	5-10	5	11.45
Digital and Computer	50	8	33.28
Refrigerator and Cooling	20-100	24	79.9
Entertainment	17-100	2	5
Cooking	40-800	1	8.33
Total	132-1060	-	137.96

The green cottage will use 138 ampere-hours daily. This estimate fits tiny cottage consumption (100 to 200 ampere-hours). The minimum support time is 408 min when consumption is 247 watts and the battery depletion is 200 amp hours at the inverter's 12-volt input voltage. When the control algorithm stops the battery from reaching 40% SOC and the backup system is linked to the grid. During economic analysis, the system's NPV, IRR, and ROI are computed. The NPV of future cash flows is computed through equation (1).

$$NPV = \mathrm{NCF}_0 + \frac{NCF_1}{(1+i)} + \frac{NCF_2}{(1+i)^2} + \frac{NCF_t}{(1+i)^t} \quad (1)$$

Where, NCF=net cash, i=discount rate, and t=financial term. NPV is positive or negative. If the net present value is 0, the designer won't care whether to do the project. At IRR, NPV is zero. Using ROI, the time at which total yearly income is computed equals the investment cost.

The statistical test is based on four-level factorial and Taguchi experimental design (irradiance, solar cell surface temperature, and wind speed). As in [29] and [30] the demand for electricity is forecasted for the following twenty-four hours using an ARMA model applied to one years of historical data from [31]. The equation (2) describes the demand model:

$$D_m(t) = \sum_{n=1}^{r} \mu_n D(t-n) + \sum_{m=0}^{s} \delta_m \varepsilon(t-m) \quad (2)$$

where $D_m(t)$ represents the current demand at living time, μ_n and δ_m are the effective coefficient and the ARMA coefficient are respectively in the demand relation, and $\varepsilon(t-m)$ equal to the prediction error coefficient. In the demand model, r values and s values cover previous errors. Using Akaike's Information Criterion, the last two parameters are determined. Term $\varepsilon(t-m)$ are computed as relative percentages of forecast error for each hour and follow a normal distribution. The hourly sun irradiance is measured at the same geographical locations. equation (3) has been used to modeled the PV in homogeneous Markov reward process.

$$PV_m(t) = \left(\frac{P_{STC}}{I_{STC}}\right)\left\{\left(x \cdot I_{M,t}\right)\left[1+\alpha\left(T_{M,t}-T_{STC}\right)\right]\right\} \quad \forall t \in \{1,2,3,\dots,23,24\} \tag{3}$$

where $PV_m(t)$ is the power of the PV, $I_{M,t}$ and $T_{M,t}$ are the solar irradiance and photovoltaic cells temperature at time (t), and P_{STC}, I_{STC} and T_{STC} are the variables of the solar power generation unit are in standard test conditions (STC). the maximum power, solar irradiance, and photovoltaic cells temperature, respectively. Lastly, x is the number of photovoltaic panels, and α represents the effective temperature coefficient in photovoltaic power loss ($^{\%}/_{°\mathrm{C}}$). To calculate the WT power from wind speed data, as was done in solar energy, the modeling is solved by predicting non-homogeneous Makove process data, and the WT power curve is converted to the analytical form shown in equation (4).

$$WT_m(t) = \begin{cases} 0 \quad for \quad s < s_{ci}, \\ Q_r \frac{s^3 - s_{ci}^3}{s_r{}^3 - s_{ci}^3} \quad for \quad s_{ci} < s < v_r, \\ Q_r \quad for \quad s_r < s < v_{co} \\ 0 \quad for \quad v > v_{co}, \end{cases}, \quad \forall t \in \{1,2,3,\dots,23,24\} \tag{4}$$

The coefficient values Q_r and s_r denote the rated power (kW) and the wind speed (m/s), whereas s_{ci} and v_{co}, and s denote the cut-in and cut-out, and wind speed, respectively. The battery bank is an element that can directly generate the electricity needed by the green cottage or be charged as a consumer by connecting to power generation sources. The state of charge (SOC) is received by HRES at any moment and displayed as a percentage. Also, equation (5) shows the BESS charging status model.

$$SOC_{BESS}(t) = SOC_{BESS}(t-1) - \begin{Bmatrix} \Delta t \cdot BESS(t) \cdot E_c & ; & BESS(t) < 0 \\ \frac{\Delta k \cdot BESS(t)}{E_d} & ; & BESS(t) > 0 \end{Bmatrix} \quad \forall t \in \{1,2,3,\dots,23,24\} \tag{5}$$

where E_c, E_d, and Δt represent the BESS charging efficiency, discharging efficiency, and sampling interval, respectively. The status of the battery power can be positive or negative. If the element works as a generator, the $BESS(t)$ will be positive and in the state of discharge, the power will be negative. Damage can be avoided if the SOC stays within a certain range, hence this range includes both the maximum and minimum values. Consequently, it needs to be in accordance with equation (6).

$$SOC_{BESS,min}(t) \leq SOC_{BESS}(t) \leq SOC_{BESS,max}(t) \quad \forall t \in \{1,2,3,\dots,23,24\} \tag{6}$$

The microgrid nonrenewable energy sources are the conventional generating units (DE). The power generated is physically constrained and represented using equations (7).

$$P_{DE,min} \leq P_{DE}(t) \leq P_{DE,max} \quad \forall t \in \{1,2,3,\dots,23,24\} \qquad (7)$$

$P_{DE,min}$ and $P_{DE,max}$ are the minimum power and maximum power of DE generator, whereas $P_{DE}(t)$ is time-dependent power of DE generator.

To compose the optimization equations, the terms of the HRES are modified. They exhibit the criteria of prediction and proportionality with time ($t \in \{1,2,\dots,24\}$). The variables indicated by $\hat{v}$ are used when the model or optimization is used in the forecasting situation. Any of the variables can qualify for this condition. For the suggested technique to MG, a optimization algorithm is implemented, comparable to the actual method of managing power grids. $\widehat{D}(t)$, $\widehat{PV}(t)$ and $\widehat{WT}(t)$ terms are related to forecasts of demand and uncontrollable Solar and wind sources in a 24-hour period. As described before, the determination of how much operationally controlled sources should contribute is determined in two distinct processes. The initial phase is termed as unit commitment (UC). It simply controls whether a unit is active or inactive. The binary variables are employed for this purpose. ED is second stage that the real power to be provided by controllable sources is determined based on the discrepancy between forecasts and actual demands.

3. Results and Discussions

Thirteen subsystem configuration possibilities were analyzed using solar-wind hybrids, batteries, and DE. In this study, the renewable energy hybrid system has a 20-year lifespan, a 16.7% discount rate, a 10% inflation rate, and meteorological data. The minimum renewable component is 23.7%. The LCOE for all subsystems combined is $0.381 per kilowatt-hour. In countries with significant inflation and discount rates, such as Iran, a 0.205 kW photovoltaic system (starting cost of 410 USD), an i500 wind turbine (beginning cost of 1000 USD), a 0.890 kW DE model TG2500DC, and two 100 ampere-hour batteries are installed. This system uses 253 liters of gasoline per year and 54% renewable energy. The DE operated for 1345 hours and generated 675 kWh. The battery stores 499 kWh annually and has a 7.03-hour compensation capacity. Table 2 demonstrates hybrid renewable energy systems' optimal combinations. According to Green Cottage Power Use, residential power consumption peaks 3 hours after sunset. On some days, electricity consumption reaches 2.09 kW. Off-hours usage was 0.01 kW. By dusk, the green cottage's yearly average power use had reached 0.47 kW.

Table 2. HRES System Architecture.

Architecture	Tg2500 (kW)	Photovoltaic (kW)	I500 (kW)	Battery (100Ah)	Investment Cost (USD)	COE (USD Per kWh)	Fuel Consumption (L)	Renewable Fraction (%)
1	0.89	0.368	0	2	1222	0.379	407	23.8

2	0.89	0.205	1	2	1888	0.381	253	54
3	0.89	0	1	3	1579	0.402	359	30
4	0.89	0	0	4	695.6	0.407	585	0
5	0.89	0.396	2	4	3378	0.446	0	100
6	0.89	0	3	5	3800	0.510	0	100
7	0.89	1.42	0	11	4130	0.547	0	0
8	0.89	0	0	0	285.46	0.636	1080	0
9	0.89	0.0065	0	5	289.83	0.637	1080	0
10	0.89	0	1	0	1278	0.721	1011	0
11	0.89	0.0035	1	0	1325	0.717	1017	0
12	0.89	0.04	14	0	14083	1.8	0	100
13	0.89	0	15	0	15000	1.91	0	100

Fig. 4 shows the green cottage's yearly electricity demand and supply. The inverter extracted 871 kWh per year from 917 kWh over 7239 operational hours. Converting AC to DC loads wastes 45.8% of energy.

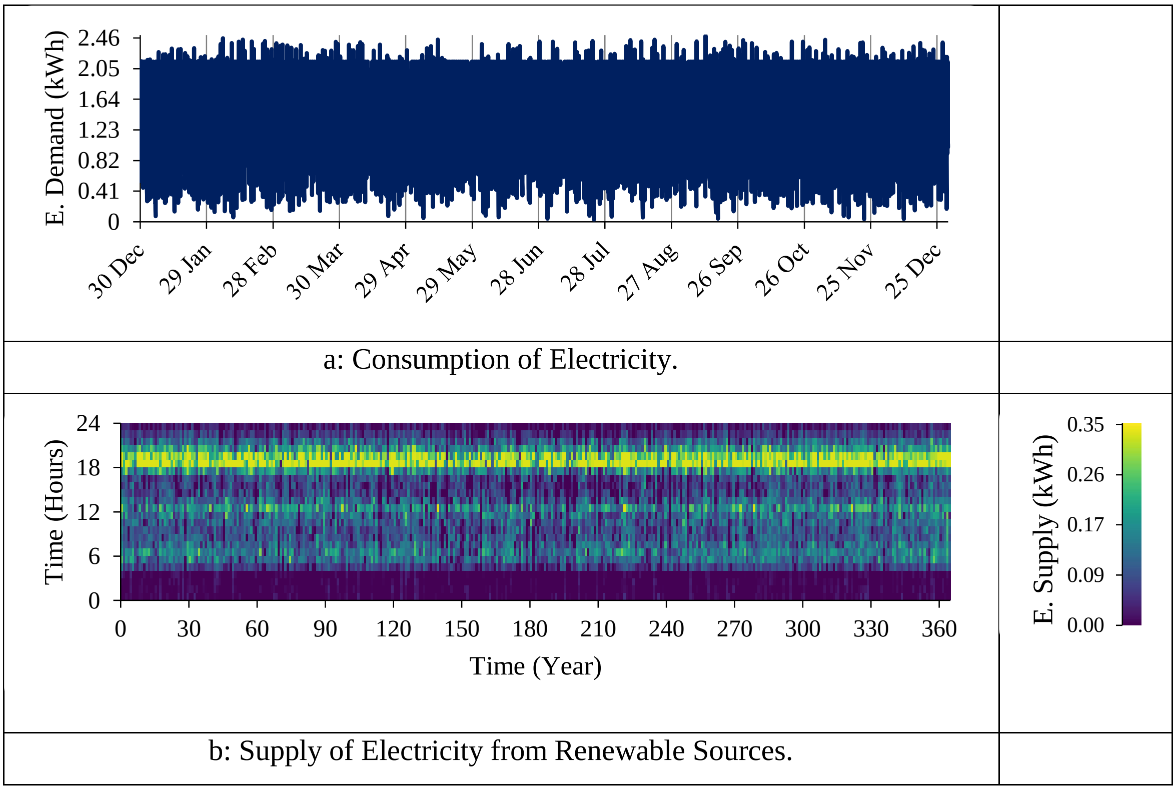

Figure 4. The Green Cottage's Annual Electricity Demand and Supply.

Each subsystem contributes a fraction to the generation of the required energy. Annually, 331 kWh are generated by the solar subsystem. The WT with high penetration equivalent to 40.8% generated 675 kilowatt-hours of energy annually and the other demand supply unit was DE with a share of 39% and annual production of 647 kilowatt-hours. System architecture No. 2 requires 253 liters of fuel, with a specific fuel demand for power output of 0.37 liters per kilowatt-hour. This unit will likewise be started 589 times a year and has a useful life of 11.2 years. There was a notional yield of 27.1%. The operation of the backup and battery energy storage subsystem is depicted in Figure 5.

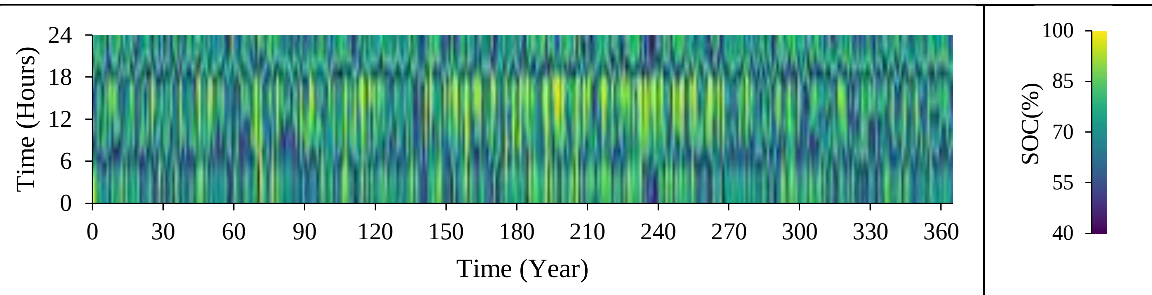

a: condition of the subsystem for energy storage.

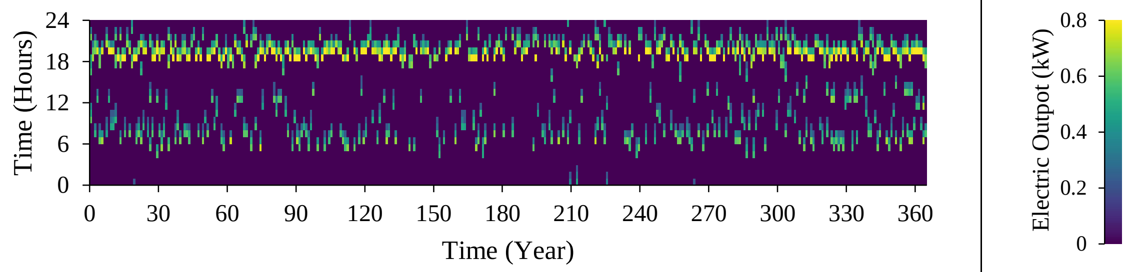

b: DE subsystem power.

Figure 5. The backup and energy storage subsystem.

The BESS installation showed that 12 volts is sufficient. BESS inputs 577 kWh and produces 446 kWh annually. Outages averaged 111 kWh per year, and batteries provided 499 kWh. The battery energy storage option can provide the green cottage's electrical needs for 7.03 hours for 0.112 USD per kilowatt-hour. The cottage's electricity use is mostly determined by its hybrid renewable energy conversion system.

Fig. 6 Shows the optimization HRES used forecasting situation and optimal hybrid energy investment value. The initial phase is termed as unit commitment and energy management under boost voltage DC-DC with predictive analytics and dynamic decision algorithm.

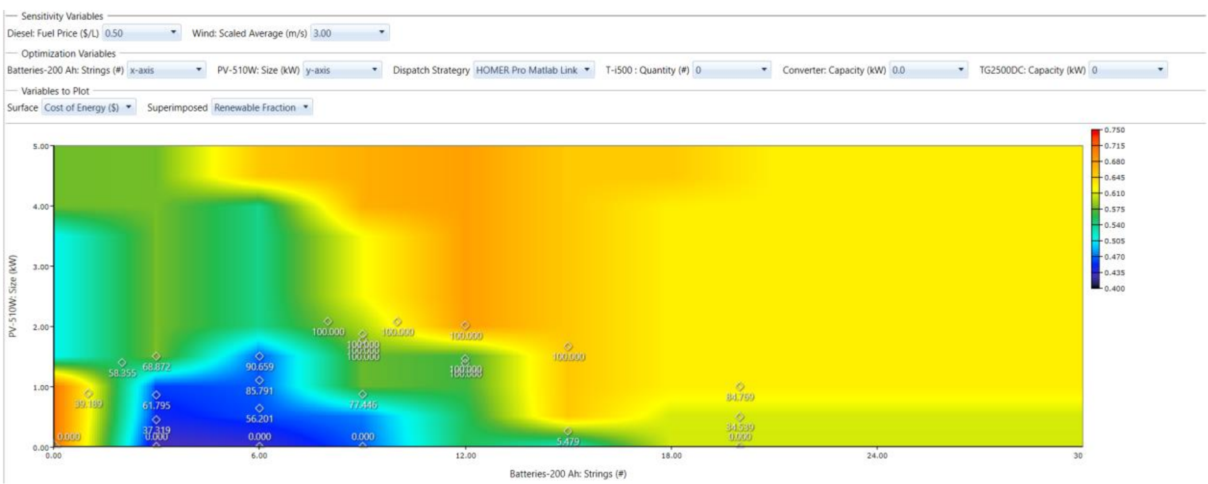

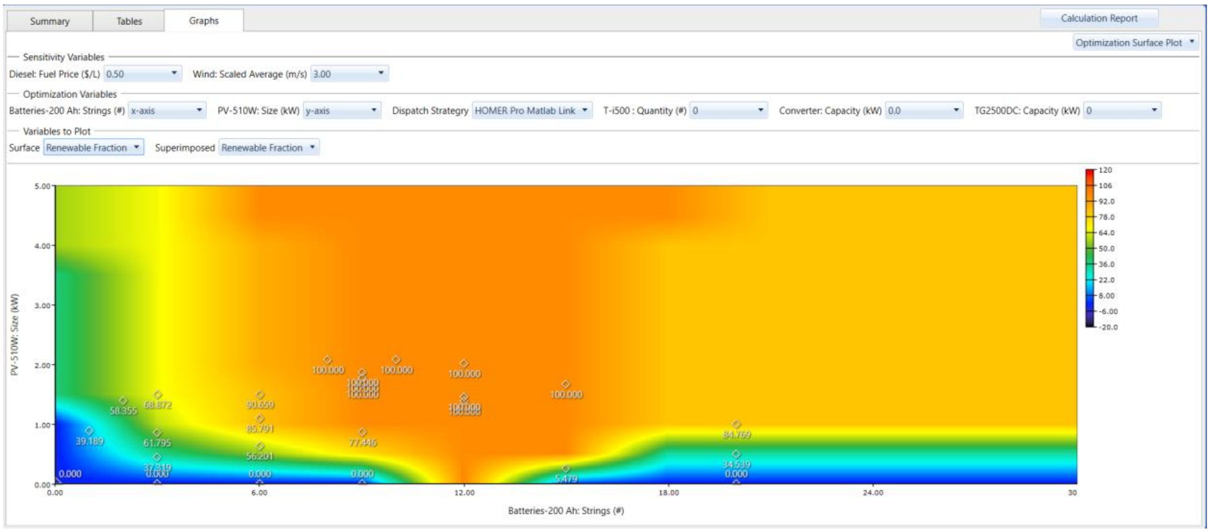
Summary
Tables
Graphs
Calculation Report
Optimization Surface Plot
Sensitivity Variables
Diesel: Fuel Price ($/L) 0.50
Wind: Scaled Average (m/s) 3.00
Optimization Variables
Batteries-200 Ah: Strings (#) x-axis
PV-510W: Size (kW) y-axis
Dispatch Strategy HOMER Pro Matlab Link
T-i500 : Quantity (#) 0
Converter: Capacity (kW) 0.0
TG2500DC: Capacity (kW) 0
Variables to Plot
Surface Renewable Fraction
Superimposed Renewable Fraction
PV-510W: Size (kW)
Batteries-200 Ah: Strings (#)

299

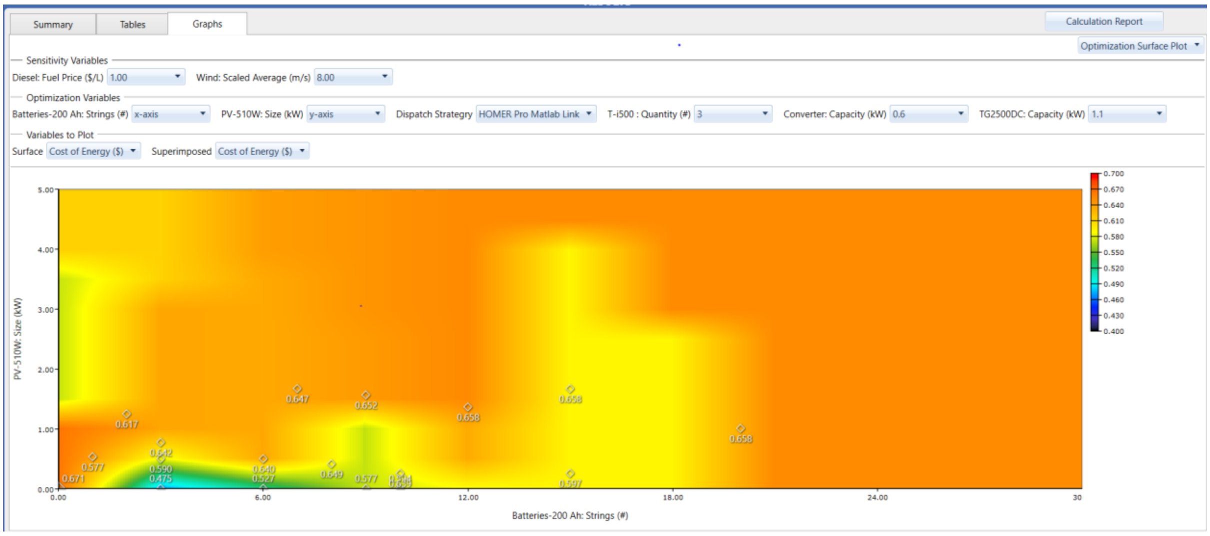
Summary
Tables
Graphs
Calculation Report
Optimization Surface Plot
Sensitivity Variables
Diesel: Fuel Price ($/L) 1.00
Wind: Scaled Average (m/s) 8.00
Optimization Variables
Batteries-200 Ah: Strings (#) x-axis
PV-510W: Size (kW) y-axis
Dispatch Strategy HOMER Pro Matlab Link
T-i500 : Quantity (#) 3
Converter: Capacity (kW) 0.6
TG2500DC: Capacity (kW) 1.1
Variables to Plot
Surface Cost of Energy ($)
Superimposed Cost of Energy ($)
PV-510W: Size (kW)
Batteries-200 Ah: Strings (#)

300


RESULTS
Summary
Tables
Graphs
Calculation Report
Optimization Surface Plot
Sensitivity Variables
Diesel: Fuel Price ($/L) 1.00
Wind: Scaled Average (m/s) 8.00
Optimization Variables
Batteries-200 Ah: Strings (#) x-axis
PV-510W: Size (kW) y-axis
Dispatch Strategy HOMER Pro Matlab Link
T-i500 : Quantity (#) 3
Converter: Capacity (kW) 0.6
TG2500DC: Capacity (kW) 1.1
Variables to Plot
Surface Renewable Fraction
Superimposed Cost of Energy ($)
PV-510W: Size (kW)
Batteries-200 Ah: Strings (#)

301

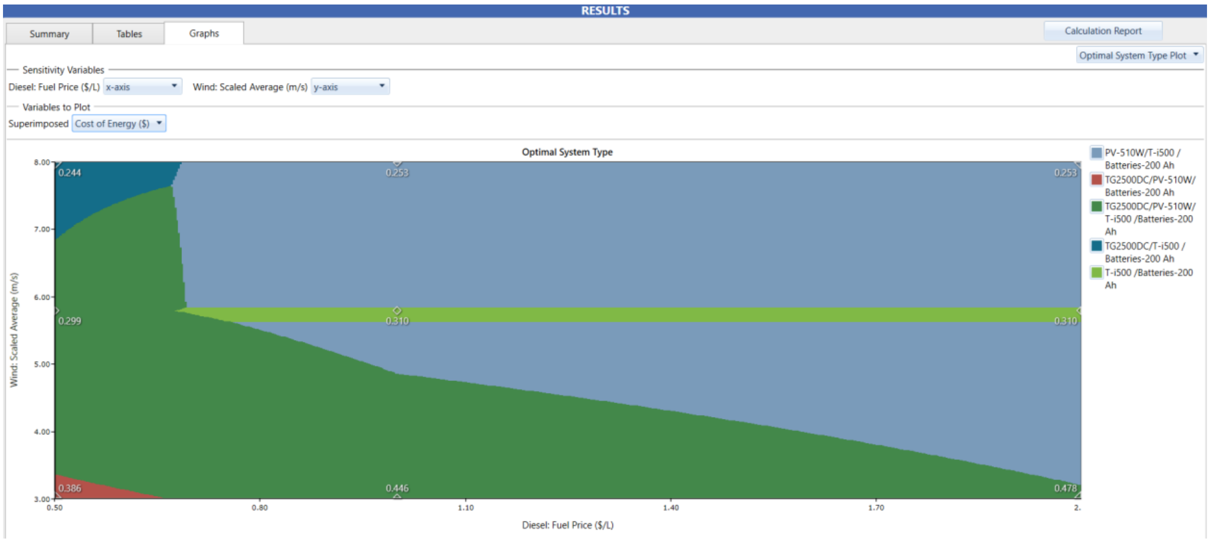

Fig. 6 displays the renewable energy fraction and net investment value utilizing a dynamic choice procedure and monthly average electric output. Average wind speed and fuel prices decrease net investment value.

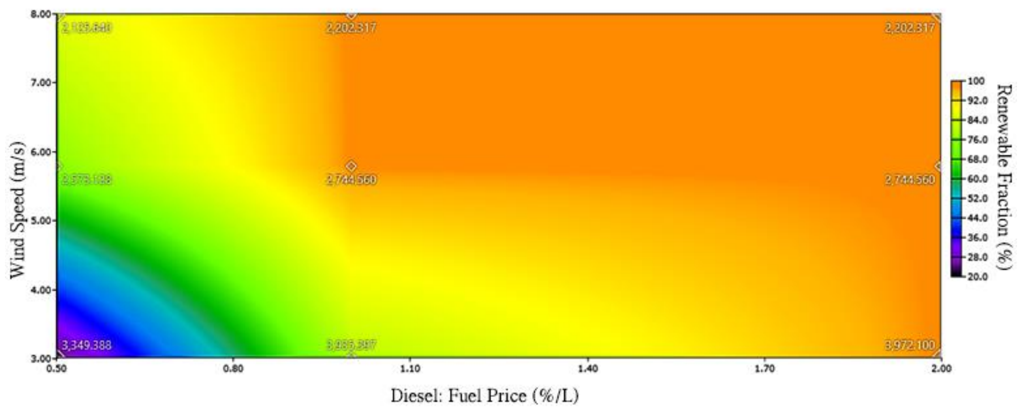

a: Renewable Energy Proportion.

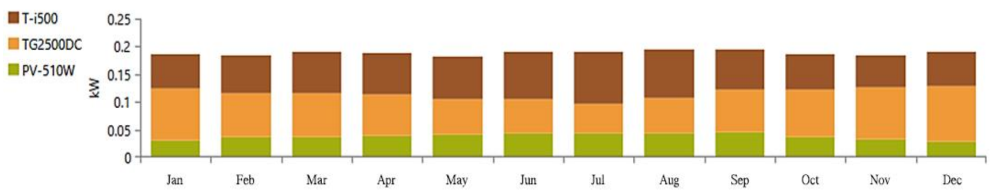

b: Economic Scenario's Monthly Average Electricity Production.

Figure 6. The percentage of renewable energy and average monthly electricity generation.

Increasing investment by more than $3,300 USD is not cost-effective and rapidly boosts the price of energy production. The development and use of a micro turbine and the lack of DE led to the use of three batteries and the expansion of the capacity of the solar and wind subsystems. This brought the price of renewable electricity down to 0.402 USD per megawatt-hour.

The cost-benefit analysis of the systems has been solved by obtaining 20-year economic data of Iran and based on the assumption of DE fuel equal to 0.12 USD and MG feed-in tariff equal to 0.05 USD with an average discount rate of 16.7%. From their commencement in 2020 until their depreciation in 2040, it is estimated that the projects will last three months. In the first scenario, the green cottage is powered for "economical" reasons. In this scenario, renewable energy accounts for 23.8% of total energy consumption, whereas nonrenewable energy accounts for 407 liters of gasoline. The second scenario, with a fuel usage of 253 liters, employs 54 percent solar and wind to accomplish the aim of being "renewable and cost-effective." The third scenario is to completely power the eco-friendly home with renewable energy. As a consequence, fossil fuels are removed, and the energy source of the eco-friendly cottage is entirely dependent on battery power. In the first scenario, the green cottage produces 1697 kWh of energy each year. In this research, following the stochastic behavior, in the practical evaluation of the systems, three progressive scenarios of High penetration of RESs were carried out with the HRES system. The first scenario has solved the basic penetration of RESs by 23.8%, the second scenario by 54%, and the third scenario by demand management as 100% of RES resources. however, Scenario 3 is not economically feasible in Iran. Despite the substantial environmental implications, this scenario should nevertheless be undertaken. Sustainable development has demonstrated that today's demands may be met with fewer fossil fuels.

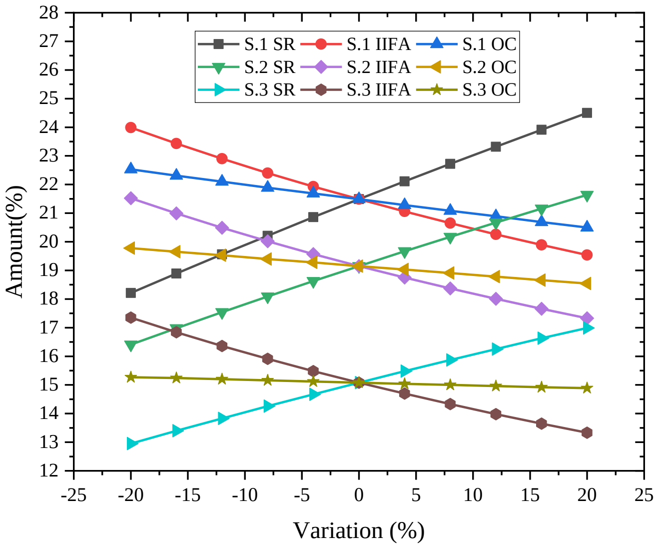

a: Analysis of sensitivity.

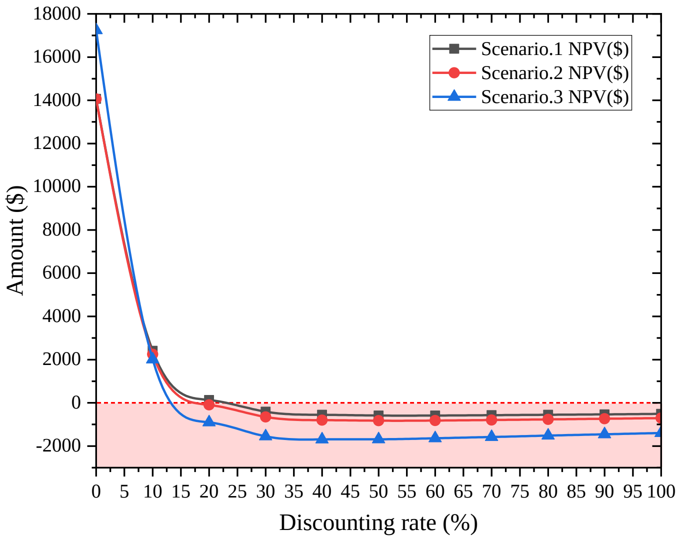

b: The impact of the discount rate on three scenarios.

Figure 7. Financial analysis of system variables.

In addition, the NPV is 553,68 US dollars, and the IRR is 21.49%. Prior to the completion of the plan to sell power to the Green Cottage in 2040, a total of $2,710.79 USD worth of energy had been acquired. In normal mode (2029), the payback period is 9.10 years, whereas in dynamic mode it is 15.71 years. The sensitivity analysis for Scenario 1 of the project reveals that the feed-in tariff has the greatest influence, followed by operational expenses, with a cost-benefit ratio of 1.38. Scenario 1 is ecologically favorable since the DE is powered by 407 liters of gasoline per year, which is equivalent to 1,065 kilos of CO_2 annually. Under the second scenario, the HRES produces 1652 kWh of energy annually. The NPV will be 341,471 US dollars, and the IRR will be 19.5%. The green cottage power revenue program ended in 2039 with total energy sales of $2,638.90 USD. In standard mode (2029), the payback period is 9.8 years; in dynamic mode, it is 17.61 years. The project's sensitivity analysis indicated that the cost-benefit ratio is 1.21, with the feed-in tariff having the most significant impact, followed by an increase in fixed assets. The use of 253,443 liters per year, which is equivalent to 633 kilos of carbon dioxide, makes Scenario 2 environmentally benign. The third scenario yields an annual energy output of 1,933 kWh. The net present value is -379.09 dollars, and the internal rate of return is 15.08%. At the conclusion of the green cottage power sales program in 2039, a total of 3,087.77 USD worth of energy had been sold. If the NPV is negative, the project is not economically justifiable and the depreciation period exceeds the life of the project. The majority of the effect is attributable to a boost in sales income, followed by an increase in fixed assets, and the implementation of this scenario does not result in greenhouse gas emissions.

According to statistical analysis of the variables influencing the system's power and performance, solar radiation with a wavelength of between 0 and 1200 $W.m^{-2}$ will always have a favorable effect on the system's power. Figure 8 depicts the impact of Environmental variables on the electrical power consumption of the green cottage. The effect of the rising sun and growing radiation intensity up to 900 W.m^{-2} has a considerable impact on the system power, while the effect of the rising sun and increasing radiation intensity up to 1200 W.m^{-2} has a smaller but positive slope. Temperature has a negative effect on the performance of solar systems, decreasing their power production by increasing their internal and external resistance. In contrast, increases in solar photovoltaic surface temperature beyond 80 degrees Celsius have a greater effect on decreasing the system's power consumption. Wind turbines with wind speeds of between 4 and 8 m/s will produce the most power. It has been established that the ideal wind speed for micro turbines (400 watts) is more than or equal to 4 m.s^{-1}.

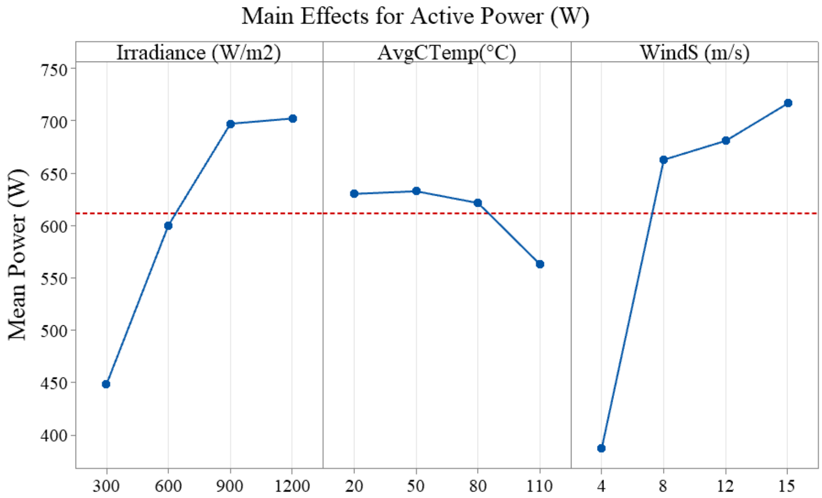

Figure 8. The average consequences of the MG's demand management.

4. Conclusions

In this article, taking into account the uncertainty of RESs and forecasting the load demand of the unit of consumption, firstly, with connecting real data, the non-homogeneous Markov model for the wind energy source and the homogeneous Markov model for the solar energy source are solved, and then the microgrid system is applied. HRES with SUC and ED terms was optimized. The results showed that forecasting models have sufficient accuracy in predicting the behavior of RESs. The green cotage MG costs are strongly affected by wind speed on any given day. Temperature caused the greatest power loss (15.8%), whereas subsystem wiring caused the least. In locations with high discount rates and low feed-in tariffs, the same as Iran, using 100% renewable electricity to supply a single-family house isn't cost-effective. Feed-in tariff increase optimizes cost-benefit analysis of HRES. NPV with a 16.7% discount rate is $70.93 and payback is 10.68 years. The crucial feed-in tariff for renewable electricity in Iran is 0.6 $ / kwh, according to a sensitivity analysis. Scenario 3 has a lower project implementation risk than 2 and 1. Therefore, green cottage's electrical supply has a lower investment cost and a significant blackout risk. HRES use three energy architecture, AC, DC, and AC/DC power supplies. The DC subsystems are connected to the DC line and include renewable energy sources [3]. These systems have the simplest renewable energy integration plan. If the inverter fails, the system will fail [4]. Paralleling low-voltage inverter connections with AC electricity solved this problem [6]. AC line hybrid system is similar DC line, except customers are directly connected to AC [5]. Most Iranians consume 220 volts at 50 Hz. In current study, the HRES has sent the green cottage's load on AC. Linear algorithms, AI, and fuzzy control are used to manage hybrid systems off-grid. Networked systems employ linear algorithms, AI, and fuzzy control. SCADA and ZigBee algorithms predict and manage energy for intelligent control systems. In these methods, hybrid systems contained a DE for optimization [8]. Dynamic control optimizes input and output ports. HRES-optimized Voltage-Based Multi-Agent Control maximized under Boost voltage. Sensing, monitoring, and analyzing voltage to determine and hybrid local multi-microgrids source voltage. Calculating the battery's measured voltage and reporting the result as a percentage. The signals voltage switching relays of sources to charge and discharge batteries and start the DE. Improved microgrid signals in the microcontroller provide non-binary, continuous battery power based on real data. In [9], SCADA was employed to manage solar, wind, fuel cell, and fixed generator energy. The source [17] presented energy data via ZigBee. Despite optimization, these systems were expensive and would shut down if a DE failed. While optimizing energy and not requiring a DE for continuous operation (using backup diesel), it has delivered power to green cottage for more than 7 hours. In [26], A 10% drop in average unit price enhanced wind power's appeal by 5.8%. The cost-benefit analysis of Iran's HRES will change with a 20% increase in feed-in tariffs to \$0.06. In [25], photovoltaic subsystems, wind, and ZigBee are suggested for buildings and homes. These systems cannot employ low voltages from renewable energy sources, and flashing has damaged certain grid. In [26], a system to monitor smart home voltage was proposed. By integrating renewable energy sources with energy management strategies, this algorithm was able to save 33% of the electricity cost during off-peak hours. In this study, 100% of green cottage's electricity demand was supplied by renewable energy sources. This system's energy production cost \$0.446/kWh. Feed-in tariffs assist low economies employ renewable energy. Lower energy costs. First scenario has 1065 kg/yr of CO2 emissions, second has 633 kg/yr.

References

[1] E. V. McLean, J. Hur, T. Whang, Renewable energy policies and household solid fuel dependence, Glob. Environ. Chang. 71 (2021) 102408. https://doi.org/10.1016/J.GLOENVCHA.2021.102408.

[2] B.O. Menyeh, Financing electricity access in Africa: A choice experiment study of household investor preferences for renewable energy investments in Ghana, Renew. Sustain. Energy Rev. 146 (2021) 111132. https://doi.org/10.1016/J.RSER.2021.111132.

[3] P. Ifaei, A. Farid, C.K. Yoo, An optimal renewable energy management strategy with and without hydropower using a factor weighted multi-criteria decision making analysis and nation-wide big data - Case study in Iran, Energy. 158 (2018) 357–372. https://doi.org/10.1016/j.energy.2018.06.043.

[4] T.K. Baul, D. Datta, A. Alam, A comparative study on household level energy consumption and related emissions from renewable (biomass) and non-renewable energy sources in Bangladesh, Energy Policy. 114 (2018) 598–608. https://doi.org/10.1016/J.ENPOL.2017.12.037.

[5] S. Hajiaghasi, A. Salemnia, M. Hamzeh, Hybrid energy storage system for microgrids applications: A review, J. Energy Storage. 21 (2019) 543–570. https://doi.org/10.1016/J.EST.2018.12.017.

[6] J. Goop, E. Nyholm, M. Odenberger, F. Johnsson, Impact of electricity market feedback on investments in solar photovoltaic and battery systems in Swedish single-family dwellings, Renew. Energy. 163 (2021) 1078–1091. https://doi.org/10.1016/j.renene.2020.06.153.

[7] L. Mellouk, M. Ghazi, A. Aaroud, M. Boulmalf, D. Benhaddou, K. Zine-Dine, Design and energy management optimization for hybrid renewable energy system- case study: Laayoune region, Renew. Energy. 139 (2019) 621–634. https://doi.org/10.1016/J.RENENE.2019.02.066.

[8] B.K. Sovacool, D.D. Furszyfer Del Rio, Smart home technologies in Europe: A critical review of concepts, benefits, risks and policies, Renew. Sustain. Energy Rev. 120 (2020) 109663. https://doi.org/10.1016/J.RSER.2019.109663.

[9] H.K. Ghritlahre, R.K. Prasad, Application of ANN technique to predict the performance of solar collector systems - A review, Renew. Sustain. Energy Rev. 84 (2018) 75–88. https://doi.org/10.1016/j.rser.2018.01.001.

[10] H. Rauf, M.S. Gull, N. Arshad, Complementing hydroelectric power with floating solar PV for daytime peak electricity demand, Renew. Energy. 162 (2020) 1227–1242. https://doi.org/10.1016/j.renene.2020.08.017.

[11] J.H. Menke, N. Bornhorst, M. Braun, Distribution system monitoring for smart power grids with distributed generation using artificial neural networks, Int. J. Electr. Power Energy Syst. 113 (2019) 472–480. https://doi.org/10.1016/j.ijepes.2019.05.057.

[12] N.A. Lee, G.E. Gilligan, J. Rochford, Solar Energy Conversion, Green Chem. (2018) 881–918. https://doi.org/10.1016/B978-0-12-809270-5.00030-3.

[13] M. Jafari, Z. Malekjamshidi, Optimal energy management of a residential-based hybrid renewable energy system using rule-based real-time control and 2D dynamic programming optimization method, Renew. Energy. 146 (2020) 254–266. https://doi.org/10.1016/j.renene.2019.06.123.

[14] M. Petrollese, G. Cau, D. Cocco, Use of weather forecast for increasing the self-consumption rate of home solar systems: An Italian case study, Appl. Energy. 212 (2018) 746–758. https://doi.org/10.1016/j.apenergy.2017.12.075.

[15] A.H. Elsheikh, S.W. Sharshir, M. Abd Elaziz, A.E. Kabeel, W. Guilan, Z. Haiou, Modeling of solar energy systems using artificial neural network: A comprehensive review, Sol. Energy. 180 (2019) 622–639. https://doi.org/10.1016/J.SOLENER.2019.01.037.

[16] H. Armghan, M. Yang, M.Q. Wang, N. Ali, A. Armghan, Nonlinear integral backstepping based control of a DC microgrid with renewable generation and energy storage systems, Int. J. Electr. Power Energy Syst. 117 (2020) 105613. https://doi.org/10.1016/j.ijepes.2019.105613.

[17] Y. He, S. Guo, J. Zhou, J. Ye, J. Huang, K. Zheng, X. Du, Multi-objective planning-operation co-optimization of renewable energy system with hybrid energy storages, Renew. Energy. 184 (2022) 776–790. https://doi.org/10.1016/J.RENENE.2021.11.116.

[18] B. Yang, J. Wang, X. Zhang, L. Yu, H. Shu, T. Yu, L. Sun, Control of SMES systems in distribution networks with renewable energy integration: A perturbation estimation approach, Energy. 202 (2020) 117753. https://doi.org/10.1016/j.energy.2020.117753.

[19] Z. Su, L. Yang, Peak shaving strategy for renewable hybrid system driven by solar and radiative cooling integrating carbon capture and sewage treatment, Renew. Energy. (2022). https://doi.org/10.1016/J.RENENE.2022.08.011.

[20] P.S. Pravin, S. Misra, S. Bhartiya, R.D. Gudi, A reactive scheduling and control framework for integration of renewable energy sources with a reformer-based fuel cell system and an energy storage device, J. Process Control. 87 (2020) 147–165. https://doi.org/10.1016/j.jprocont.2020.01.005.

[21] G. Human, G. van Schoor, K.R. Uren, Genetic fuzzy rule extraction for optimised sizing and control of hybrid renewable energy hydrogen systems, Int. J. Hydrogen Energy. 46 (2021) 3576–3594. https://doi.org/10.1016/j.ijhydene.2020.10.238.

[22] X. Dong, J. Lu, B. Sun, Min-max Operation Optimization of Renewable Energy Combined Cooling, Heating, and Power Systems Based on Model Predictive Control, IFAC-PapersOnLine. 53 (2020) 12809–12814. https://doi.org/10.1016/j.ifacol.2020.12.1956.

[23] E. Noghreian, H.R. Koofigar, Power control of hybrid energy systems with renewable sources (wind-photovoltaic) using switched systems strategy, Sustain. Energy, Grids Networks. 21 (2020) 100280. https://doi.org/10.1016/j.segan.2019.100280.

[24] A. V. Mercedes Garcia, F.J. Sánchez-Romero, P.A. López-Jiménez, M. Pérez-Sánchez, A new optimization approach for the use of hybrid renewable systems in the search of the zero net energy consumption in water irrigation systems, Renew. Energy. 195 (2022) 853–871. https://doi.org/10.1016/J.RENENE.2022.06.060.

[25] O.R. Llerena-Pizarro, R.P. Micena, C.E. Tuna, J.L. Silveira, Electricity sector in the Galapagos Islands: Current status, renewable sources, and hybrid power generation system proposal, Renew. Sustain. Energy Rev. 108 (2019) 65–75. https://doi.org/10.1016/J.RSER.2019.03.043.

[26] S. Kallio, M. Siroux, Exergy and exergo-economic analysis of a hybrid renewable energy system under different climate conditions, Renew. Energy. 194 (2022) 396–414. https://doi.org/10.1016/J.RENENE.2022.05.115.

[27] S. Tamjid Shabestari, A. Kasaeian, M.A. Vaziri Rad, H. Forootan Fard, W.M. Yan, F. Pourfayaz, Techno-financial evaluation of a hybrid renewable solution for supplying the predicted power outages by machine learning methods in rural areas, Renew. Energy. 194 (2022) 1303–1325. https://doi.org/10.1016/J.RENENE.2022.05.160.

[28] M.D. Leonard, E.E. Michaelides, Grid-independent residential buildings with renewable energy sources, Energy. 148 (2018) 448–460. https://doi.org/10.1016/J.ENERGY.2018.01.168.

[29] K. Bhatia, R. Mittal, J. Varanasi, M.M. Tripathi, An ensemble approach for electricity price forecasting in markets with renewable energy resources, Util. Policy. 70 (2021) 101185. https://doi.org/10.1016/J.JUP.2021.101185.

[30] F.E. Riaño, J.F. Cruz, O.D. Montoya, H.R. Chamorro, L. Alvarado-Barrios, C.: Riaño, F.E.; Cruz, J.F.; Montoya, O.D.; Chamorro, H. Ali, J.F.C. Co, Reduction of Losses and Operating Costs in Distribution Networks Using a Genetic Algorithm and Mathematical Optimization, Electron. 2021, Vol. 10, Page 419. 10 (2021) 419. https://doi.org/10.3390/ELECTRONICS10040419.

[31] M.E. Shayan, G. Najafi, B. Ghobadian, S. Gorjian, M. Mazlan, M. Samami, A. Shabanzadeh, Flexible Photovoltaic System on Non-Conventional Surfaces: A Techno-Economic Analysis, Sustain. 2022, Vol. 14, Page 3566. 14 (2022) 3566. https://doi.org/10.3390/SU14063566.